This article has been accepted for publication in a future issue of this journal, but has not been fully edited. Content may change prior to final publication. Citation information: DOI 10.1109/LAWP.2018.2882584, IEEE Antennas and Wireless Propagation Letters

An Optically Transparent Broadband Microwave Absorber using Interdigital Capacitance

Harsh Sheokand, Gaganpreet Singh, Saptarshi Ghosh, *Member, IEEE*, J. Ramkumar, *Senior Member, IEEE*, S. Anantha Ramakrishna, and Kumar Vaibhav Srivastava, *Senior Member, IEEE*

***Abstract*—In this paper, an optically transparent broadband microwave absorber has been developed. The proposed geometry is constructed of patterned resistive films of ITO on flexible substrates, such that the structure exhibits broadband absorptivity (above 90%) from 4 to 17.20 GHz (covering C, X, and Ku bands). The novelty of the design lies in leveraging the properties of interdigital capacitance to achieve wide absorption (fractional bandwidth of 124.53%), angular stability, as well as optical transparency compared to the earlier reported broadband absorbers. Moreover, the structure has been extensively investigated through deriving an equivalent circuit model and studying surface current distributions. Experimental validation of the fabricated prototype has also confirmed the potential use of resistive film based broadband absorbers in several applications.**

Index Terms*— *Circuit analog absorber; broadband absorber; optically transparent absorber; interdigital capacitance

I. Introduction

ABSORPTION of electromagnetic (EM) wave in the microwave spectrum has been a subject of notable practical importance since many decades. Significant efforts have been devoted to design absorber structures capable of being deployed in practical applications such as radar cross section reduction, EM interference, EM compatibility, wireless communication, imaging devices, and so forth [1]-[3]. One of the earliest radar absorbers, Salisbury Screen [4], is based on single resistive sheet placed a quarter-wavelength above a conductive surface. However, the geometry, although simple in design, suffers from narrow bandwidth. The bandwidth was later improved through developing the Jauman absorber [5], but at the expense of increased thickness and larger weight. Other techniques, such as Dallenbach absorbers, carbon nanotubes, pyramidal absorbers have also limited applications due to their bulky nature and fragility [6], [7].

With the emergence of the concept of circuit analog (CA), absorbing structures have been realized with large bandwidth and reduced thickness [8]-[13]. This CA absorber is made of a periodic resistive-conductive pattern imprinted on a single-/multi-layered dielectric substrate, often terminated by a ground plane. By choosing appropriate parameters for the top surface resistive pattern, broadband absorption occurs for the range of frequencies where the grounded dielectric and top surface susceptances cancel each other. This finite resistance can be implemented by either mounting lumped resistors [8], [9], or coating resistive ink [10], [11], or using resistive sheets [12], [13]. However, the former technique suffers from complex fabrication procedures, high cost, and/or limited accuracy. On the contrary, the latter techniques based on resistive layers, can be thought of as a good alternative due to high accuracy, ease of fabrication, and low cost.

In this paper, a polarization-insensitive optically transparent broadband microwave absorber has been presented based on CA concept. The novelty of the proposed structure lies in its utilization of interdigital capacitive structures to efficiently modulate the top surface admittance. This optimizes the impedance match leading to a significant increase in the absorption bandwidth as compared to existing broadband absorbers. Moreover, the structures are made on commercially available Indium-tin-oxide (ITO) resistive films on flexible polymer sheets, such that the overall structure behaves as an optically transparent broadband microwave absorber. This optically transparent characteristic can be exploited in several practical applications, such as touch panel control, RFID system, solar cells, and transparent RF devices. They can also be implemented as observation windows in EM shielding rooms, and electronic surveillance. The proposed structure is also analyzed by deriving equivalent circuit models and parametric variations. Excimer Laser micromachining technique has been used to fabricate the design. The measured response shows good agreement with the simulated responses.

II. Design and Analysis

Fig. 1 depicts the unit cell geometry of the proposed broadband absorber. The top and bottom surfaces are comprised of ultra-thin (~1000 Å) resistive films (having different values of surface resistance) deposited on flexible substrates, and are separated from each other by an air spacer. ITO is used as the resistive film due to its commercial availability, low cost, as

Manuscript submitted on --, revised on --, accepted on --.

This work was supported in part by DRDO, India, under Project No. RCI/DCMM/LPD-I/CARS/0385.

Harsh Sheokand, Saptarshi Ghosh, and Kumar Vaibhav Srivastava are with the Department of Electrical Engineering, Indian Institute of Technology Kanpur, Uttar Pradesh 208016, India (email: mail.harsh90@gmail.com; joysaptarshi@gmail.com; kvs@iitk.ac.in).

Gaganpreet Singh, and J. Ramkumar are with the Department of Mechanical Engineering, Indian Institute of Technology Kanpur, Uttar Pradesh 208016, India (email: gaganprt@iitk.ac.in; jrkumar@iitk.ac.in).

S. Anantha Ramakrishna is with the Department of Physics, Indian Institute of Technology Kanpur, Uttar Pradesh 208016, India (email: sar@iitk.ac.in).

This article has been accepted for publication in a future issue of this journal, but has not been fully edited. Content may change prior to final publication. Citation information: DOI 10.1109/LAWP.2018.2882584, IEEE Antennas and Wireless Propagation Letters

well as optical transparency. Top surface ITO film is periodically patterned in the shape of a square loop with equally spaced fingers protruding inwards to generate interdigital capacitance (IDC) with laterally shifted fingers of the same width protruding outwards from a square ITO patch. Four additional square patches are added to reduce the comparatively large gaps in the corners. The bottom resistive film is a continuous one (without any pattern). The supporting substrate in both cases is a Polyethylene Terephthalate (PET) sheet (ε_r = 3.2 and $tan\ \delta$ = 0.003) having a thickness (t_p) of 0.175 mm.

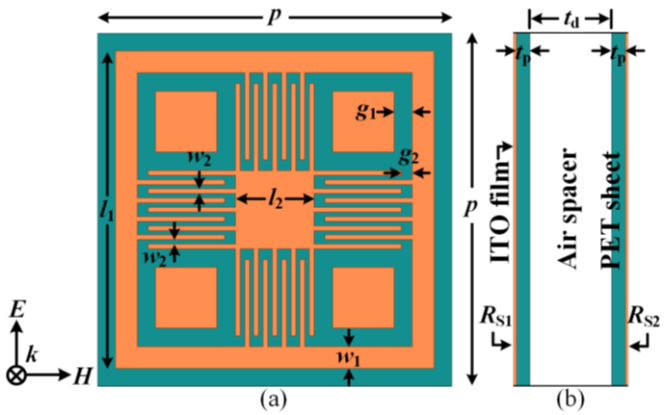

Fig. 1. Unit cell layout of the proposed broadband absorber. (a) Top view, and (b) side view. The optimized dimensions are: p = 16.2 mm, l_1 = 14.6 mm, l_2 = 3.6 mm, w_1 = 1 mm, w_2 = 0.2 mm, g_1 = 0.85 mm, g_2 = 0.5 mm, t_d = 5.65 mm, t_p = 0.175 mm, R_{S1} = 35 Ω/□, and R_{S2} = 10 Ω/□.

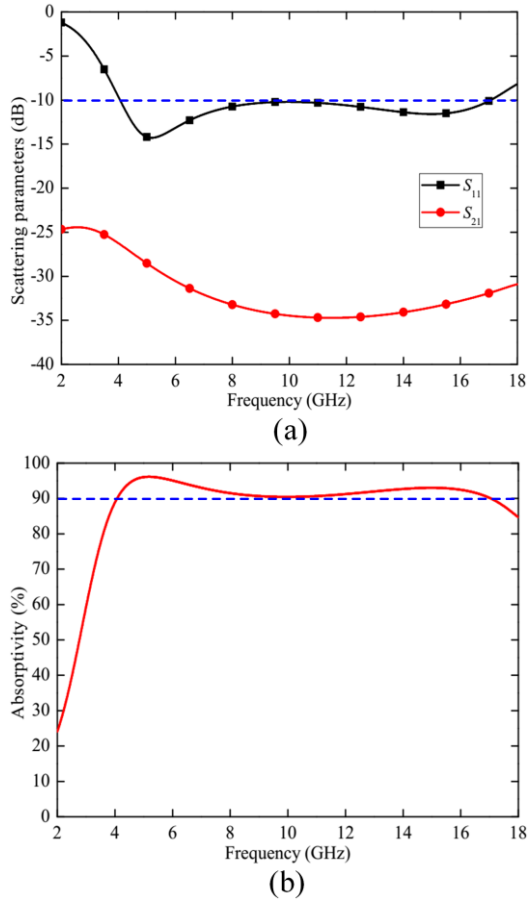

Fig. 2. Simulated (a) scattering parameters, and (b) absorptivity of the proposed broadband absorber.

The unit cell layout of the proposed design has been numerically simulated in Ansys HFSS software, using periodic boundary conditions. Figure 2(a) depicts the scattering parameters in which reflection coefficient (S_{11}) is found to be below -10 dB from 3.97 to 17.24 GHz, whereas transmission coefficient (S_{21}) is well below -25 dB throughout the frequency spectrum. This low value of S_{21} can be attributed to small surface resistance (10 Ω/□) of the bottom ITO film, which may be approximated as a reflector. Thus, the overall absorptivity ($A = 1 - |S_{11}|^2 - |S_{21}|^2$) of the structure is obtained to have value above 90% over the frequency range of 4 to 17.20 GHz as shown in Fig. 2(b). The design exhibits a fractional bandwidth of 124.53% with a center frequency of 12.6 GHz, thereby covering the entire C, X, and Ku bands in the microwave range.

To elucidate the broadband absorption obtained from the proposed design, the structure has been examined for intermediate configurations, as illustrated in Fig. 3. When only the IDC element is analyzed, the geometry exhibits near-unity absorption, but for a smaller frequency range. The bandwidth has been enhanced by incorporating the outer square loop in the structure; however the absorptivity level reduces below 90%. Later, four square patches have been integrated in the final design, which results in an increased level of absorptivity (while maintaining the bandwidth almost constant).

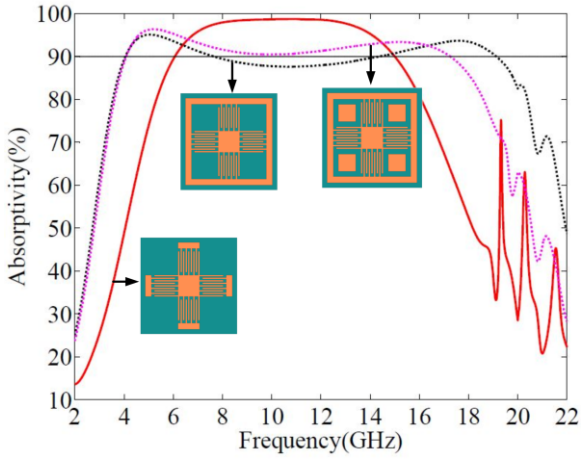

Fig. 3. Simulated absorptivity responses of the proposed broadband absorber for different intermediate configurations.

The above inference has further been confirmed while studying the electric field and surface current distributions of the broadband absorber. Figures 4(a) and (b) depict the electric field intensity of the proposed structure at the absorption peaks, viz. 5.17 and 15 GHz, respectively, showing higher amount of field localization and enhancement between the IDC fingers. It is also observed from surface current density shown in Figs. 4(c) and (d) that the square patches have no significant effect at the lower resonance (5.17 GHz) in contrast to its profound impact at higher absorption frequency (15 GHz). These square patches, operating as an intermediate bridge between the outer square loop and the inner IDC element, allow EM wave propagation at higher frequencies (corresponding to smaller wavelengths). Thus, the absorption bandwidth as well as the absorptivity value of the structure can be precisely controlled with the square loop dimensions and/or their positions.

This article has been accepted for publication in a future issue of this journal, but has not been fully edited. Content may change prior to final publication. Citation information: DOI 10.1109/LAWP.2018.2882584, IEEE Antennas and Wireless Propagation Letters

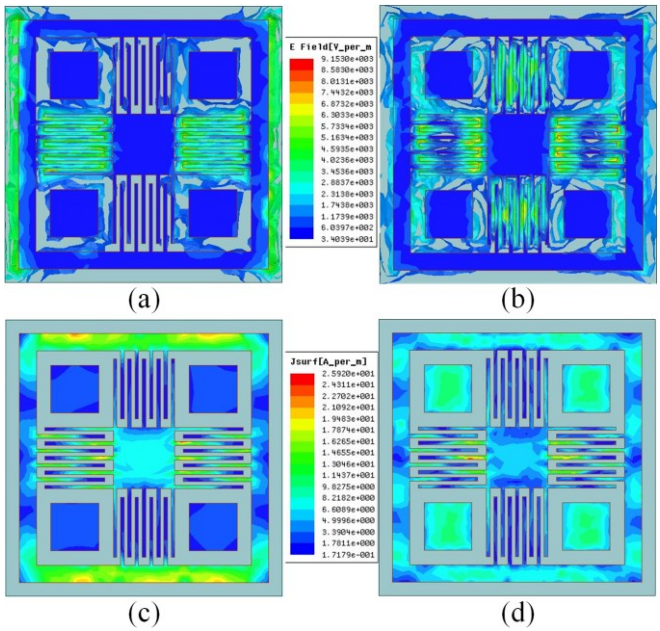

Fig. 4. Simulated magnitude of electric field intensity at (a) 5.17 GHz, and (b) 15 GHz and surface current density at (c) 5.17 GHz, and (d) 15 GHz of the proposed broadband absorber.

To illustrate the effect of the ITO resistive films, the absorption response of the proposed structure has been studied for different values of the top layer surface resistance (R_{S1}). It is observed from Fig. 5 that with increasing top layer resistance, the two absorption peaks move towards each other. This increases the overall absorption level, but simultaneously reduces the absorption bandwidth. Therefore, 35 Ω/□ has been selected as the optimum surface resistance, thus resulting in the widest absorption bandwidth (above 90%). Figure 5 also indicates that the broadband absorption primarily occurs owing to high ohmic loss of the resistive film, since the design has insignificant dielectric loss (because of the use of air spacer).

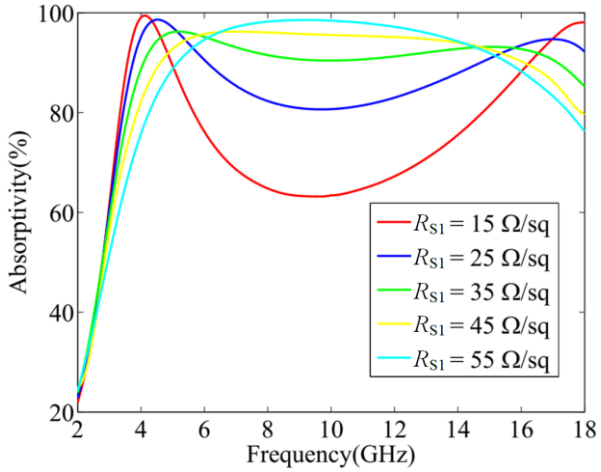

Fig. 5. Simulated absorptivity of the proposed structure for different values of the top layer surface resistance (R_{S1}).

An equivalent circuit model has been presented in Fig. 6(a) to further illustrate the absorption mechanism of the proposed structure. Top surface is characterized by a parallel combination of resistance-inductance-capacitance, while the dielectric substrate and the bottom surface are modelled as a transmission

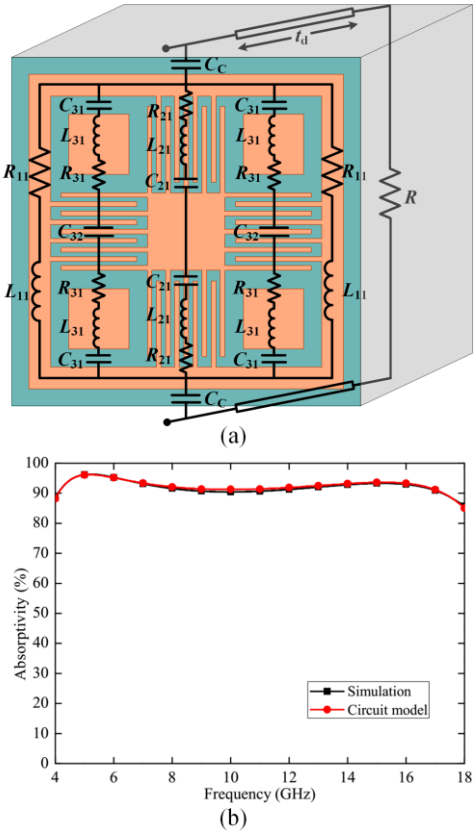

Fig. 6. (a) Equivalent circuit model of the proposed absorber, and (b) comparison of absorptivity calculated from equivalent circuit model and obtained from full wave simulations in HFSS.

line segment (of thickness t_d) and an equivalent resistance (R), respectively. Owing to small resistance value, the transformed impedance of the ground plane approximately reflects an inductive (capacitive) response at low (high) frequency in parallel with the top circuit components [14]. The series circuits R_{21}-L_{21}-C_{21}, at the top surface, represent the IDC element along the electric field orientation (assuming in vertical direction). R_{11} and L_{11} denote the outer square loop resistances and inductances, respectively, while R_{31}-L_{31}-C_{31} model the alternating path through the square patches. The intermediate capacitance across the IDC element in the alternating path has been indicated by C_{32}. Coupling capacitance between the neighboring unit cells has also been incorporated as C_C in the circuit design. This circuit model has been implemented in Advanced Design System (ADS) software and hybrid optimization tool is used to match the circuit calculated response with that of the numerically simulation. The values of the lumped parameters are then determined as follows: R_{11} = 500 Ω, L_{11} = 2.2 nH, R_{21} = 125 Ω, L_{21} = 2.45 nH, C_{21} = 140 pF, R_{31} = 25 Ω, L_{31} = 17.3 nH, C_{31} = 5.2 fF, C_{32} = 8.7 fF, C_C = 0.6 pF and R = 13 Ω, using curve fitting technique. The absorptivity value obtained from the circuit model is also compared with the simulated response as shown in Fig. 6(b), and they are found to be in good agreement, thus validating the proposed circuit model.

The proposed design has four-fold symmetry and therefore results in reasonably polarization-insensitive behavior (not shown here due to brevity). Further, the structure has the

This article has been accepted for publication in a future issue of this journal, but has not been fully edited. Content may change prior to final publication. Citation information: DOI 10.1109/LAWP.2018.2882584, IEEE Antennas and Wireless Propagation Letters

advantage of high angular stability as compared to the earlier reported broadband absorbers. The geometry, being convoluted due to presence of the IDC elements, provides compactness as well as less dependence on the incident angle [15]. Under TE polarization, the structure exhibits absorption bandwidth (above 85%) from 4.5 to 18 GHz at 40° angle of incidence, as depicted in Fig. 8(a). On the contrary, the absorption bandwidth gradually shifts to higher frequency range, during TM polarization, as shown in Fig. 8(b).

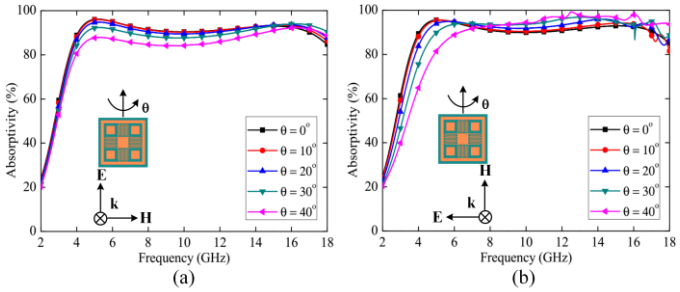

Fig. 7. Simulated absorptivity of the proposed structure for different incident angles under (a) TE polarization, and (b) TM polarization.

III. Experimental Verification

To experimentally demonstrate the proposed absorber, the structure is fabricated using commercially available ITO resistive films deposited on PET sheets. The top resistive film (R_{S1} = 35 Ω/□) is patterned by ablating the ITO coating using micromachining by excimer laser (Coherent Variolas Copres Pro 205F) [15], whereas the bottom layer is a continuous resistive film (R_{S2} = 10 Ω/□). The top and bottom sheets are stretched and taped over a 5 mm thin acrylic frame (as 5.65 mm acrylic was unavailable) to form air spacer. The frame is made of an inner cross and an outer square loop, both having minimal widths, such that the ITO films can be spread flat without any bending. A 26.2 cm × 26.2 cm sample consisting of 16 × 16 unit cells is fabricated as shown in inset of Fig. 8. The detailed fabrication procedure has been discussed in Refs. [16], [17].

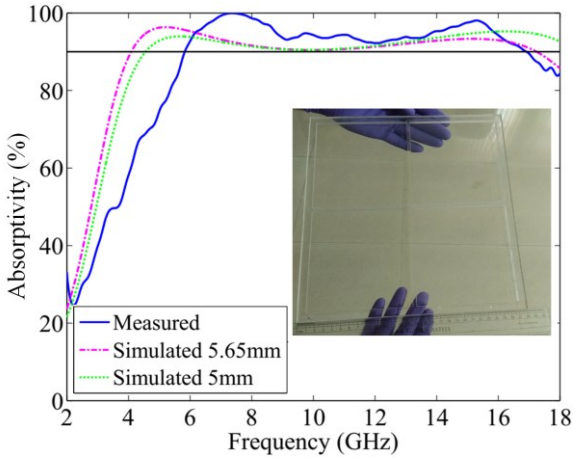

Fig. 8. Comparison of measured and simulated absorptivity of the proposed broadband absorber. The simulation results are shown for two different thickness of air spacer t_d = 5 mm and 5.65 mm. Inset shows the photograph of the fabricated absorber sample.

The fabricated prototype was measured in an anechoic chamber, using free space technique [18]. The reflectance was normalized with respect to an identical dimensional copper plate, whereas the transmission was calibrated with respect to free space. Two broadband horn antennas (1-18 GHz) and a network analyzer were used to measure the transmission and reflection coefficients of the sample. Far field condition was properly maintained while positioning the antennas [19]. Pyramidal foam absorbers were kept surrounding the prototype to prevent any unwanted spillover past the edges of the sample and minimize the edge effects throughout the measurement [20], [21]. The absorption was finally determined from the reflected and transmitted spectrum.

The measured absorptivity has been presented in Fig. 8, which shows the absorption level above 90% over the frequency range of 5.8- 17 GHz under normal incidence. As the fabricated sample has 5 mm thin air spacer, the simulation has been re-performed for 5 mm thin air spacer for comparison purpose (the original proposed structure had 5.65 mm thin air spacer). The measured response has a similar spectral shape, although the lower frequency edge is shifted to higher frequencies. This shift arises possibly due to (i) variation of resistance of the ITO film from the optimal parameters across the sheet area, (ii) slight sag of the free PET sheet areas in between the supporting acrylic structure, (iii) limited size of the fabricated sample and the diffraction effects at low-frequency, and (iv) inclusion of acrylic frame to support the ITO films.

TABLE I. Comparison with other transparent broadband absorbers (λ_g is the guided wavelength corresponding to dielectric constant ε_r)

Absorber structure	Centre frequency (GHz)	-10dB bandwidth in GHz (%)	Dielectric constant (ε_r)	Thickness (λ_g)
[17]	10.36	8.6 (83.01%)	1	5 (0.173 λ_g)
[22]	12.85	9.1 (70.8%)	2.25	3.85 (0.247λ_g)
[23]	11.5	7 (60.87%)	2.65	2.55 (0.157λ_g)
[24]	16.5	14 (84.84%)	3	5.5 (0.524λ_g)
Proposed	**10.60**	**13.2 (124.53%)**	**1**	**5.65 (0.2λ_g)**

IV. Conclusion

In this paper, a polarization-insensitive optically transparent broadband absorber based on interdigital capacitive resonators has been presented. The proposed structure exhibits a significantly larger absorption bandwidth with respect to the earlier reported broadband absorbers, as shown in Table I. The structure also provides compactness and angular stability owing to use of IDC elements. Moreover, the design is made of resistive films and air spacer, thereby realizing an optically transparent microwave absorber. Polarization-insensitivity, experimental demonstration, and mechanical flexibility are the additional benefits that make the proposed design suitable for various practical applications.

ACKNOWLEDGMENT

The authors are grateful to Ms. Kajal Chaudhari (Ph.D. research scholar, Department of Materials Science and Engineering, IIT Kanpur, India) for her help in measurement of the ITO sheet resistances using four-probe method.

REFERENCES

[1] E. F. Knott, J. F. Shaeffer, and M. T. Tuley, *Radar Cross Section*, Raleigh, NC, USA: SciTech, 2004, second edition.

[2] A. Fallahi, A. Yahaghi, H.-R. Benedickter, H. Abiri, M. Shahabadi, and C. Hafner, "Thin wideband radar absorbers," *IEEE Trans. Antennas Propag.*, vol. 58, no. 12, 4051-4058, 2010.

[3] G. Dayal, and S. A. Ramakrishna, "Design of multi-band Metamaterial Perfect Absorbers with stacked metal-dielectric disks," *J. Opt.*, vol. 15, p. 055106, 2013.

[4] W. W. Salisbury, "Absorbent body of electromagnetic waves," U. S. patent 2,599,944, Jun. 10, 1952.

[5] L. J. Du Toit, "The design of Jauman absorbers," *IEEE Antennas Propag. Mag.*, vol. 36, no. 6, pp. 17-25, 1994.

[6] M. Park, J. Choi, and S. Kim, "Wide bandwidth pyramidal absorbers of granular ferrite and carbonyl iron powders," *IEEE Trans. Magn.*, vol. 36, no. 5, pp. 3272–3274, 2000.

[7] Y. Naito, and K. Suetake, "Application of ferrite to electromagnetic wave absorber and its characteristics," *IEEE Trans. Microw. Theory Tech.*, vol. 19, no. 1, pp. 65–72, 1971.

[8] Y. Shang, Z. Shen, and S. Xiao, "Frequency-selective rasorber based on square-loop and cross-dipole arrays," *IEEE Trans. Antennas Propag.*, vol. 62, no. 11, pp. 5581–5589, Nov. 2014.

[9] S. Ghosh, S. Bhattacharyya, and K. V. Srivastava, "Design, characterisation, and fabrication of a broadband polarization-insensitive multilayer circuit analogue absorber," *IET Microw. Antennas Propag.*, vol. 10, no. 8, pp. 850-855, 2016.

[10] F. Costa, A. Monorchio, and G. Manara, "Analysis and design of ultrathin electromagnetic absorbers comprising resistively loaded high impedance surfaces," *IEEE Trans. Antennas Propag.*, vol. 58, no. 5, pp. 1551–1558, 2010.

[11] S. N. Zabri, R. Cahill, and A. Schuchinsky, "Compact FSS absorber design using resistively loaded quadruple hexagonal loops for bandwidth enhancement," *Electron. Lett.*, vol. 51, no. 2, pp. 162-164, 2015.

[12] G. Dayal, and S. A. Ramakrishna, "Broadband infrared metamaterial absorber with visible transparency using ITO as ground plane," *Opt. Exp.*, vol. 22, no. 12, pp. 15104-15110, 2014.

[13] Y. Okano, S. Ogino, and K. Ishikawa, "Development of optically transparent ultrathin microwave absorber for ultrahigh-frequency RF identification system," *IEEE Trans. Microw. Theory Tech.*, vol. 60, no. 8, pp. 2456-2464, 2012.

[14] F. Costa, A. Monorchio, and G. Manara, "Analysis and design of ultrathin electromagnetic absorbers comprising resistively loaded high impedance surfaces," *IEEE Trans. Antennas Propag.*, vol. 58, no. 5, pp. 1551–1558, May 2010.

[15] S. Sheikh, "Miniaturized-element frequency-selective surfaces based on the transparent element to a specific polarization," *IEEE Antennas Wireless Propag. Lett.*, vol. 15, pp. 1661-1664, Sept. 2016.

[16] Govind Dayal, S. A. Ramakrishna, S.N. Akhtar and J. Ramkumar, "Excimer laser micro-machining using binary mask projection for large area structuring with single micron features," *J. Micro- Nano-Manufacturing (ASME)* ***1***, Art. No. 031002 (2013).

[17] H. Sheokand, S. Ghosh, G. Singh, M, Saikia, K. V. Srivastava, J. Ramkumar, and S. A. Ramakrishna "Transparent broadband metamaterial absorber based on resistive films," *J. Appl. Phys.*, vol. 122, 105105, 2017.

[18] S. Ghosh, and K. V. Srivastava, "An angularly stable dual-band FSS with closely spaced resonances using miniaturized unit cell," *Microw. Wireless Compon. Lett.*, vol. 27, no. 3, pp. 218-220, Mar. 2017.

[19] C. A. Balanis, *Antenna Theory: Analysis and Design*, 1st ed. New York, USA: Wiley, 2005.

[20] D. Ferreira, R. F. S. Caldeirinha, I. Cuiñas, and T. R. Fernandes, "Tunable square slot FSS EC modelling and optimization," *IET Microw. Antennas Propag.*, vol. 11, no. 5, pp. 737-742, 2017.

[21] H. Li, C. Yang, Q. Cao, and Y. Wang, "An ultrathin bandpass frequency selective surface with miniaturized element," *IEEE Antennas Wireless Propag. Lett.*, vol. 16, pp. 341-344, 2017.

[22] C. Zhang, Q. Cheng, J. Yang, J. Zhao, and T. J. Cui, "Broadband metamaterial for optical transparency and microwave absorption," *Appl. Phys. Lett.*, vol. 110, p. 143511, 2017.

[23] K. Chen, L. Cui, Y. J. Feng, J. M. Zhao, T. Jiang, and B. Zhu, "Coding metasurface for broadband microwave scattering reduction with optical transparency," *Opt. Exp.*, vol. 25, no. 5, pp. 5571-5579, 2017.

[24] D. Hu, J. Cao, C. Zhang, T. Wu, Q. Li, Z. Chen, Y. Wang, and J. Guan, "Optically transparent broadband microwave absorption metamaterial by standing-up closed-ring resonators," *Adv. Opt. Mat.*, p. 1700109, 2017.